Production and applications of positron microbeams

1989 J. Phys.: Condens. Matter 1 SA135

(http://iopscience.iop.org/0953-8984/1/SA/019)

J. Phys.: Condens. Matter 1 (1989) SA135–SA143. Printed in the UK

Production and applications of positron microbeams

G R Brandes†, K F Canter†, T N Horsky†, P H Lippel† and A P Mills Jr‡

† Brandeis University, Waltham, Massachusetts 02254, USA

‡ AT&T Bell Laboratories, Murray Hill, New Jersey 07974, USA

Received 28 November 1988

Abstract. The production of a positron microbeam using the high-brightness beam developed at Brandeis University and possible applications of this microbeam to spatially resolved defect studies and positron microscopy are reviewed. The high-brightness beam consists of a W(110) primary moderator and two remoderation stages which provide a 500-fold increase in brightness. With this brightness increase and microbeam optics, we are able to form a 12 μm FWHM beam (48 mrad pencil half-angle) at 5 keV beam energy. The well characterised small-diameter beam is particularly adaptable for determining defect concentration and structure, both laterally and in a depth-profiling mode. In the case of a transmission positron microscope or a positron re-emisssion microscope operating in a high-magnification mode, efficient image formation requires the use of a microbeam to maximise the number of positrons in the area being imaged. Results of the scanning microbeam tests and the application of a microbeam to positron microscopy and defect studies are reviewed.

The recent development of high-brightness monoenergetic slow-positron beams allows us to extend positron studies of the solid state to a spatially resolved mode. The production, application and results of two types of apparatus to achieve this end are reviewed. The first is the positron microbeam which directly exploits the positron beam brightness and may be used to study small objects such as whiskers, cracks, voids and field emission tips and to map the positronic properties of a sample surface. The second is the positron microscope, which utilises a microbeam to illuminate a portion of the sample to be imaged. Positron microscopy, particularly positron re-emission microscopy (PRM), offers the ability to observe and study materials directly in a unique manner.

The technique of obtaining slow positrons of a few electronvolts from a solid surface irradiated by β-decay or pair production positrons is well known (for an up-to-date review of positron interactions near a surface see [1]). A moderator, which is either a metal crystal that has a negative affinity for positrons [2, 3] or an insulator that has a long diffusion length for hot (electronvolt energy) positrons [4, 5], is placed in close proximity to the positron source. A beam several millimetres in diameter (determined by the source–moderator configuration) of nearly monoenergetic positrons results. A practical positron microbeam or microscope requires maximisation of the number of positrons obtained from this moderator in a small-diameter beam. Although the positron beam diameter may be reduced with apertures, the attendant loss of flux usually makes this an undesirable method. Consequently, the basis for these devices is a bright source of low-energy positrons. Brightness is a measure of how well a beam of charged particles

0953-8984/89/SA0135 + 09 $02.50

can be collimated and/or focused to a small diameter at a particular energy [6]. As first pointed out in [7], brightness can be increased by accelerating and focusing the beam to between 0.1 and 0.01 of the original moderator diameter onto the surface of another moderator (a 'remoderator'). A large fraction of the positrons thermalise and are re-emitted from this small spot. This method of circumventing Liouville's theorem relies on the same non-phase space-conserving processes involved in the primary slow-positron beam production.

The first brightness-enhanced beam was reported [8] and used two stages of reflection mode remoderation, achieving a factor of 50 in brightness enhancement. The Brandeis beam (see [9] and references therein) employs two stages of weak-focusing reflection mode brightness enhancement and achieves a factor of 500 in brightness enhancement. A fraction of the positrons emitted from the 10 mm W(110) primary moderator are ultimately re-emitted from a region 0.13 ± 0.02 mm in diameter of a W(110) moderator, referred to as the 'second remoderator' after two stages of brightness enhancement. Although 94% of the slow positrons emitted from the primary moderator are lost in the process, the resulting flux emitted from second remoderator is 500 times greater than the flux that would be obtained by just aperturing the primary moderator to this diameter. The brightness per volt of the Brandeis beam is 1.3×10^8 e^+ s^{-1} cm^{-2} rad^{-2} V^{-1} [10]† with a primary ^{58}Co source strength of 100 mCi. Future improvements in the first remoderator purity should double the present 500-fold brightness enhancement.

Another approach to brightness enhancement, which is easier from the optics point of view but more difficult from the materials science point of view, is transmission mode brightness enhancement. This method was originally avoided because of the difficulty of obtaining self-supporting thin (about 1000 Å) single-crystal metal films. Now that these films are becoming readily available‡ this approach may be considered as feasible. Further improvement to either mode of brightness enhancement may be achieved by the introduction of cooling at the remoderation stages. In [11] it was suggested that the transverse energy spread of the re-emitted positrons decreases as kT, and while there may be a lower limit [12] to this, one may still be able to pick up an additional factor of 5 in the brightness at each stage.

To probe the surface and near-surface region of a sample, the final beam energy will typically be a few kiloelectronvolts [13–15]. By accelerating the positrons emitted from the second remoderator of the Brandeis beam to this energy, Liouville's theorem allows one to obtain, in principle, a beam a few micrometres in diameter, i.e. a microbeam. The addition of transport optics and a short-focal-length lens to the brightness-enhanced beam is all that is required [10]. Although this appears to be a trivial modification, further stages of spot size reduction eventually produce practical problems owing to the small size of the apparatus and the greater effect of lens aberrations.

To investigate electrostatic lenses, we may use the third-order trajectory equation of an axially symmetric system which may be obtained by including terms of third order in both r and dr/dz and terms including third order in the series expansion of the electric field [16, 17]. From this expression, aberration effects may be investigated for particular electrostatic lenses. While this leads to a complete treatment of the third-order aberrations (coma, distortion, sperical aberration, astigmatism and curvature of field), it is not in a form which lends itself to easy use. Consequently a simplified but adequate

† The brightness per volt of the positron beam is incorrectly reported in [10]. The correct brightness per volt is as stated in this paper.

‡ Single-crystal thin films are available from J Chevallier, University of Aarhus, Denmark.

treatment of aberrations, which allowed for the use of the existing first-order optics computer routines, was incorporated into our design procedure.

The final unaberrated spot size d_f may be expressed as

$$d_f = (d/\theta_f)\sqrt{E_T/E_f}$$

where d is the positron moderator emitting area, E_T is the positron transverse energy component, and θ_f and E_f are the final pencil half-angles and energy [6]. A correction to this first-order expression may be determined by considering spherical aberration. Spherical aberration has received the most attention of the five third-order aberrations because it restricts resolving power and spot definition and tends to be the dominant aberration. The final spot diameter d_f, including a spherical aberration expression, is given by [10]

$$d_f = (d/\theta_f)\sqrt{E_T/E_f} + c_s D\theta_f^3/4$$

where D is the diameter of the two-tube lens and c_s is the dimensionless spherical aberration constant whose value is determined by the lens (typically $100 \leqslant c_s \leqslant 250$ for two-tube lenses [16, 18]). The spherical aberration contribution varies linearly with the tube diameter D of the final lens and, consequently, D should be made as small as possible. By taking the derivative of this formula with respect to θ_f, we can find the pencil half-angle for obtaining the smallest final spot diameter at a particular E_f. If we assume the trajectories before the last gap are parallel to the symmetry axis, the image pencil half-angle may be expressed as $\theta_f = \varepsilon/2L$, where ε is the fraction of the lens filled at the last gap and LD is the lens-gap-to-sample length. The parameter L or ε may be adjusted to meet experimental criteria or incident beam characteristics. The largest factor in reducing the spot size is E_T for the second remoderator. To improve this requires the replacement of the tungsten crystal with a Ni single crystal and/or the cooling of this second remoderator. Using $E_T \simeq 0.2$ eV (W(110) moderator), $d = 100\ \mu$m, $c_s = 100$ and $D = 1500\ \mu$m, the minimum spot size d_f is 32 μm, 17 μm and 13 μm for final beam energies of 1 keV, 5 keV and 10 keV, respectively. If we change to a Ni(100) moderator, which has $E_T \simeq 0.04$ eV, the final spot diameters are 17 μm, 9 μm and 7 μm for final beam energies of 1 keV, 5 keV and 10 keV, respectively. It should be noted that this formula is useful for determining the optimal pencil half-angles and minimum attainable spot size even when brightness enhancement is not used.

The first demonstration [10] of a positron microbeam utilised the Brandeis beam; figure 1 illustrates the pertinent details of how the microbeam was produced and observed. Positrons are transported to a micro-two-tube (MTT) lens which not only focuses the beam down to a small spot but also was designed to have a rastering capability. The arrangement of lenses used to transport from the second remoderator gun up to the two-tube lens were designed using Gaussian optics with aberrations contributing only a few per cent in the beam spread. However, at the final stage of focusing by the MTT, aberrations play a significant role and the expression discussed above was used in the design and operation of the lens. A grid mesh with square cells having bar widths of 25 μm and hole widths of 40 μm was mounted on a linear manipulator to test the scanning microbeam. The positron microbeam was rastered across the grid by varying the potential of opposing sectors symmetrically about the final potential. A NaI detector was used to detect annihilation γ-rays, positrons annihilating at the grid bar being detected with far greater efficiency than those passing through the grid and annihilating beyond the grid and out of direct view of the detector. As shown in figure 2, the beam can be rastered without degradation up to 250 μm from the axial position by applying a

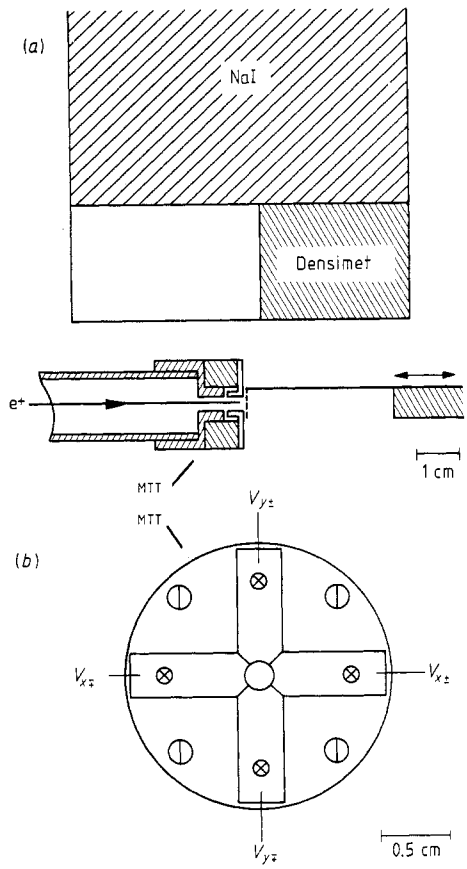

Figure 1. (*a*) Schematic diagram of the scanning positron microbeam test configuration. Positrons incident from the left are brought to a focus by the MTT lens and are rastered across a test grid mounted on a linear manipulator. (*b*) The segmentation of the MTT lens, necessary for rastering the positron microbeam, is shown in end view. The beam is rastered by varying symmetrically the potential (about the final potential) placed on opposing segments.

potential between V_F and $V_F \pm 300$ V on opposing segments for this grid position. By reversing the potential the beam could be rastered an equivalent distance in the opposite direction, allowing one to study a region 500 μm in diameter.

The full line in figure 2 is a simulated scan produced by rastering a 7 μm $\times$ 55 μm uniform-density spot across the mesh. The smaller dimension is in the direction of rastering which is along one of the symmetry axes of the mesh array. The longer dimension of the rectangular spot is oriented 55° with respect to the rastering direction. Although a range of spot sizes could be fitted to the one-dimensional scans, a rectangular beam profile was needed to account for scans obtained at right angles as well as an observed maximum transition of 75% through the mesh. The distorted shape of the microbeam was attributed to aberrations incurred by poorly centring the incident beam on the condensing lens axis.

Another microbeam lens constructed for the Brandeis positron re-emission microscope (discussed later in this paper) did not have the segmented feature of this lens but utilised a set of deflectors before the lens to ensure incident beam alignment. A symmetric

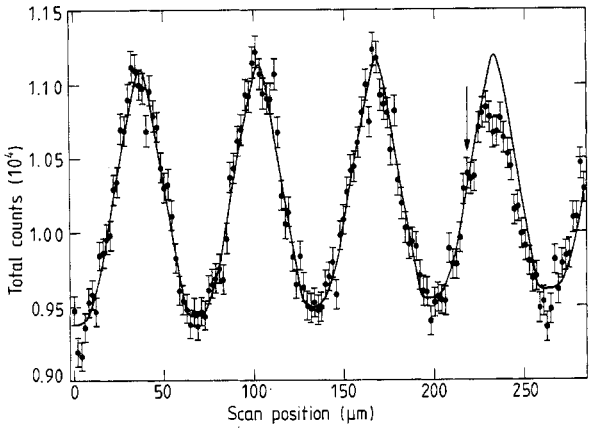

Figure 2. Positron microbeam scan in which the beam is rastered 280 μm from the axial position across a square test grid with bar widths of 25 μm and hole widths of 40 μm: ——, fit to the data from 0 to 220 μm produced in simulation by rastering a 7 μm × 55 μm beam profile across the mesh. The poor fit beyond 220 μm is attributed to a mesh irregularity. Up to the arrow, the fit produced $\chi^2/\nu = 151/101$. The background is 6.7×10^3 in this 200 s/point scan.

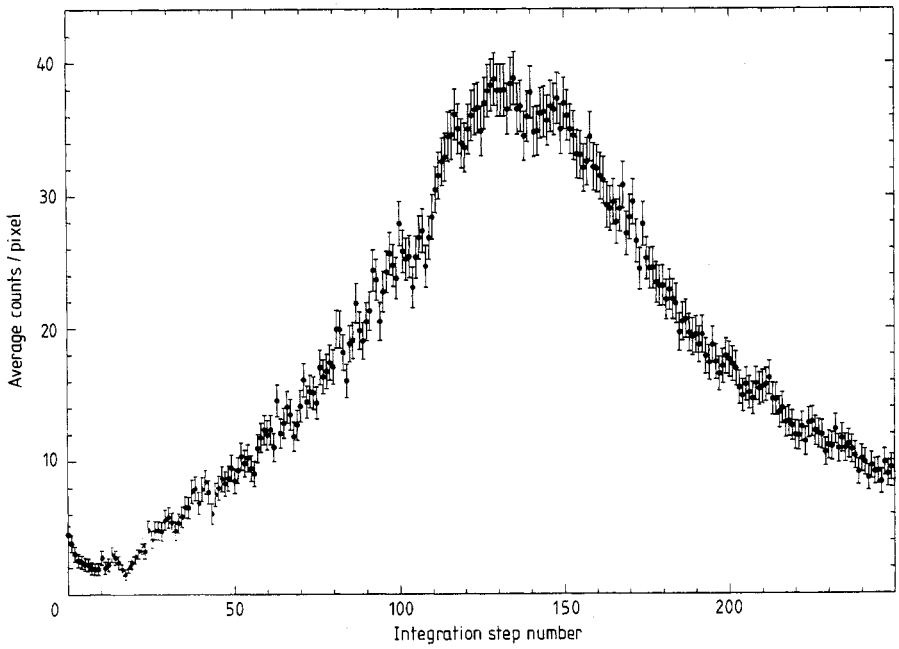

Figure 3. A slice through the centre of an image of the positron microbeam demonstrating its 12 μm FWHM. One step equals 1300 Å = 130 nm.

spot is easily obtained since direct imaging of the microbeam with the positron re-emission microscope facilitated tuning the beam within several hours instead of the several days required with the mesh rastering method. Figure 3 shows a section through

an image of the 5 kV beam, demonstrating its 12 μm FWHM, 25 μm beam diameter, in good agreement with the predicted spot size.

Further spot size reduction—beyond that which can be achieved by improving brightness of the positron beam remoderators—requires an additional stage of brightness enhancement or the incorporation of line-focusing schemes. Line focusing such as that suggested in [19] results in a much narrower width in one dimension (but greater width in the other) than can be achieved through cylindrical focusing. In [19] a lens was modelled which consists of two sets of offset parallel cylinders at different voltages and which is predicted to reduce an infinitely bright beam 0.1 mm in diameter to 100 Å. While positron moderators are not infinitely bright, they have sufficient phase space to achieve 1000 Å beam widths which may be scanned across the sample. By continued rotation and scanning of the sample, information on the microstructure may be obtained in all directions.

One of the more obvious uses of a microbeam would be to extend the wealth of positron studies carried out to date to samples restricted to a small size. Bench-top beams would be particularly adaptable to defect studies in a depth-profiling mode [13–15] as well as determining defect concentrations with respect to lateral position with about 1 μm resolution. Lateral defect resolution on the micrometre scale, combined with typically attainable 0.10 μm depth resolution, might make a scanning defect microprobe ideal for ascertaining degrees of crystallinity and interfacial defects [20]. The defect sensitivity of a scanning positron microbeam may also prove to be a valuable complement to the metallographic and microscopic techniques presently used in the microelectronics industry. With a high-flux facility, we could expand the defect studies, which are a measure of positron trapping, to include measurements of the electronic momentum density of the sample by means of the angular correlation of annihiltion radiation measurements [21]. This capability would add an enormous amount of information for distinguishing the various types of positron-trapping sites (e.g. monovacancies, grain boundaries and misfit dislocations at interfaces) in a spatially resolved mode. It is important to emphasise that even with further minimisation of the spot diameter the resolution of the microprobe will still be limited by the diffusion length–lateral implantation width of the positron.

Structures in or on a sample smaller than the beam diameter–implantation profile may be investigated by forming a magnified image of the transmitted or re-emitted positrons. Here the microbeam is essential to concentrate positrons in a small area in order to form a magnified image in a reasonable period of time. Of several contributions to the resolution of a positron microscope there is a counting-statistics-limited term proportional to $J^{-1/2}$ which is important to minimise (J being the flux density). With brightness enhancement, J may be increased with only a small decrease in total intensity. While one might be able to obtain a comparable flux density by using a higher-flux positron beam, a few orders of magnitude of the flux would be wasted if one did not employ brightness enhancement.

The first microscope to use positrons was the transmission positron microscope [22], which is the direct analogue of the existing transmission electron microscopes. In [22] it was suggested that because of the opposite sign of the Coulomb interaction comparison of the contrast differences between transmission electron microscopy (TEM) and transmission positron microscopy (TPM) images could help to isolate the effects of particular terms in the scattering cross section. Also, TPM combined with secondary-electron analysis techniques should provide different sensitivity to target composition from that of TEM. Since the magnitudes of these effects are greater at low energies (kiloelectronvolts), this device would benefit from the implementation of microbeams.

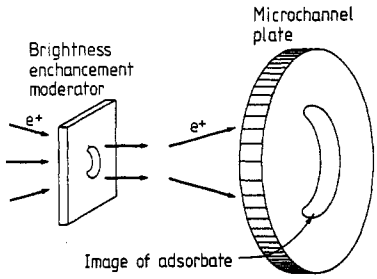

Figure 4. Schematic diagram from [23], showing the positron re-emission microscope principle. A fraction of the positrons implanted in the sample thermalise, diffuse to the surface and are re-emitted, and a magnified image is formed. Contours of adsorbates on the surface will also be imaged by the low-energy positrons.

The positron re-emission microscope was first proposed in [23]† and operates on a principle fundamentally different from those employed in existing microscopes. In the positron re-emission microscope, positrons are implanted at kiloelectronvolt energies into a sample having a negative positron affinity, and those which thermalise and are emitted from the surface are imaged (see figure 4). While the positron re-emission microscope has its antecedent in the thermionic emission microscope, and while there are also photo-excited negative-affinity electron-emitting surfaces, there is at present no direct analogue of this microscope. Contrast in the re-emitted positron image can be provided by non-uniform film thickness, bulk and surface defects, patches of different crystal orientations, contaminant layers that affect φ_+ and hence the emission probability, adsorbed molecules or larger structures that attenuate the emitted positrons, and material differences (different φ_+).

We have constructed [25, 26] a positron re-emission microscope in which the positrons are accelerated to 5 keV with a lens (MTT) 1.5 mm in diameter and are capable of being brought to a focus 25 μm in diameter (12 μm FWHM) onto a sample. Positrons which diffuse to the opposite side and are re-emitted are magnified with a three-element cathode lens, magnified further by a projector lens (low-distortion einzel lens) and projected onto a channel electron multiplier array coupled to a position-sensitive two-dimensional resistive anode readout. The first demonstration of this mode of operation involved defocusing the incident beam and using just the objective lens to form a 330× image of the shadow of a fine mesh. The mesh was placed over a polycrystalline Ni foil and, consequently, was back illuminated with about 1 eV (work function) positrons re-emitted from the Ni foil. This demonstrated that it was possible to image a region of the foil greater than 100 μm × 100 μm without noticeable distortion and with a resolution of better than 1 μm.

The full positron re-emission microscope was recently reported [26]; an 1150× magnification and 300 ± 100 nm resolution, comparable with the optical resolution limit, was demonstrated. The sample was a free-standing Ni(100) crystal 1500 Å thick grown by evaporation onto a NaCl crystal. The film was floated off the substrate and back-supported on a hexagonal mesh measured to have 108 μm openings (diameter of an inscribed circle) and 20 μm bar widths. The Ni crystal was annealed in vacuum prior to installation in the microscope. Figure 5 shows an 1150× image of a portion of the film.

† Note that the direct electron analogue of the positron re-emission microscope could be obtained using a negative-affinity electron-emitting sample (see, e.g. [24]).

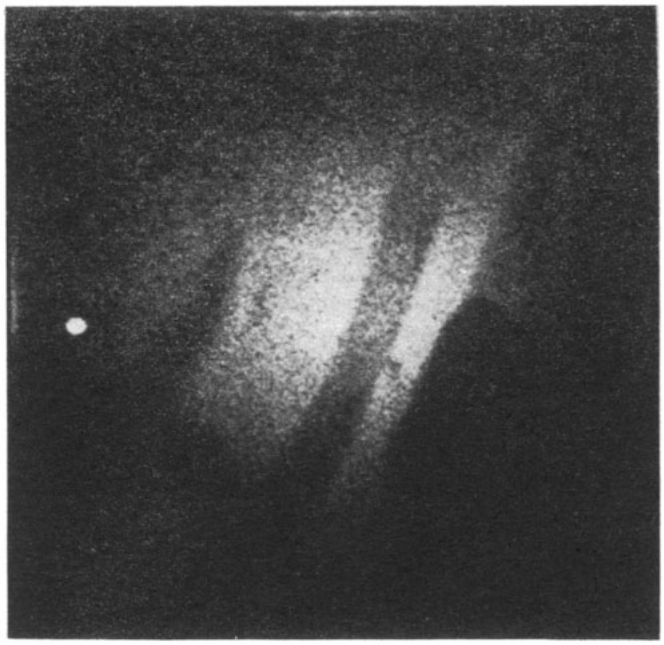

Figure 5. 1150× PRM image of defect structures in Ni foil. The dark angled region in the lower left is the edge of the support grid. The whitest areas correspond to 40 counts/pixel (256 × 256 pixels for the entire frame), with the exception of the detector hot spot on the centre left area of the detector. The dark noise is 0.1 counts h^{-1}/pixel.

Because of the manner of preparation of the sample, variations in the Ni film thickness are probably not responsible for the contrast evident in figure 5. Annealing *in situ* drastically alters the finger-like structures.

Dislocations [27], which are present even in well annealed materials (typically about 10^7 cm^{-2}), may be introduced at a high density when the crystal is grown or when strain is applied. When a strained specimen is annealed at a moderate temperature, dislocations tend to become ordered, resulting in small-angle or tilt boundaries. We thus find it reasonable to assume that the different patches of emissivity are due to the trapping of positrons at different rates by various boundaries parallel to the surface of the material. We expect larger tilt angles to result in more trapping and hence to correspond to darker areas on the PRM image. Surface contamination could also contribute to some of the observed emission variations. A subsequent 120 keV TEM examination of the film showed some areas of the film (after rough handling when transferring from the positron re-emission microscope to the transmission electron microscope) that had finger-like areas of close-packed dislocation lines.

Bringing kiloelectronvolt positrons in from the front of the sample for subsurface defect studies would be invaluable since PRM would not be restricted to thin (about 100 nm) samples. Reports of the construction and demonstration of a positron re-emission microscope which utilises this mode of operation with a magnification of 56× and a resolution of 2300 μm have been given in [28, 29]. The defect sensitivity of the microscope was demonstrated by showing the differences between the contrast of sputtered and annealed regions of a sample. The feasibility of imaging biological specimens is also claimed. The difficulty with reflection geometry is that bringing posi-

trons in off axis requires weak fields which seriously degrades PRM resolution. Furthermore, implementing a short-focal-length lens for a microbeam will be difficult owing to the restrictive geometry. Normal incidence, such as in the reflection low-energy electron microscope [30, 31], might circumvent this difficulty but requires more aperturing than can be afforded with today's positron fluxes.

Acknowledgments

This work is supported in part by National Science Foundation Grant DMR 8519524 and National Institute of Health Grant BRSGS07RR-07044.

References

[1] Schultz P J and Lynn K G 1988 *Rev. Mod. Phys.* **60** 701
[2] Pendayala S, Bartell L D, Girouard F E and McGowen J W 1974 *Phys. Rev. Lett.* **33** 1031
[3] Mills A P Jr, Platzman P M and Brown B L 1978 *Phys. Rev. Lett.* **41** 1076
[4] Canter K F, Coleman P G, Griffith T C and Heyland G R 1972 *J. Phys. B: At. Mol. Phys.* **5** L167
[5] Mills A P Jr and Gullikson E M 1986 *Appl. Phys. Lett.* **49** 1121
[6] Canter K F and Mills A P Jr 1982 *Can. J. Phys.* **66** 551
[7] Mills A P Jr. 1980 *Appl. Phys.* **23** 189
[8] Frieze W E, Gidley D W and Lynn K G 1985 *Phys. Rev.* B **31** 5628
[9] Canter K F, Brandes G R, Horsky T N, Lippel P H and Mills A P Jr 1987 *Atomic Physics with Positrons* 1st edn (London: Plenum)
[10] Brandes G R, Canter K F, Horsky T N, Lippel P H and Mills A P Jr 1988 *Rev. Sci. Instrum.* **59** 228
[11] Fischer D A, Lynn K G and Gidley D W 1986 *Phys. Rev.* B **33** 4479
[12] Gullikson E M, Mills A P Jr, Crane W S and Brown B L 1985 *Phys. Rev.* B **32** 5484
[13] Trifthauser W and Kogel G 1982 *Phys. Rev. Lett.* **48** 1741
[14] Lynn K G, Frieze W E and Vehanen A 1983 *Phys. Rev.* B **27** 6626
[15] Bentzon M D, Huomo H, Vehanen A, Hautojarvi P, Lahtinen J and Hautala M 1987 *J. Phys. F: Met. Phys.* **17** 1477
[16] Grivet P 1972 *Electron Optics* 2nd edn (Oxford: Pergamon)
[17] Spangenberg K R 1948 *Vacuum Tubes* 1st edn (New York: McGraw-Hill)
[18] Klemperer O and Wright W D 1939 *Proc. Phys. Soc.* B **51** 296
[19] Daglish R L, Winchester T and Smith A M 1983 *Nucl. Instrum. Methods* **218** 7
[20] Schultz P J, Lynn K G, Frieze W E and Vehanen A 1983 *Phys. Rev.* B **27** 6626
[21] Berko S 1983 *Positron Solid State Physics,* ed. W Brandt and A Dupasquier (Amsterdam: North-Holland) p 64
[22] Van House J and Rich A 1988 *Phys. Rev. Lett.* **60** 169
[23] Hulett L D, Dale J M and Pendyala S 1984 *Mater. Sci. Forum* **2** 133
[24] Drouhin H J, Hermann C and Lampel G 1985 *Phys. Rev.* B **31** 3859
[25] Brandes G R, Canter K F, Horsky T N and Mills A P Jr 1988 *Appl. Phys.* **46** 335
[26] Brandes G R, Canter K F and Mills A P Jr 1988 *Phys. Rev. Lett.* **61** 492
[27] Corish J 1985 *Defects in Solids* ed. A V Chadwick and M Terenzi (London: Plenum) pp 1–50
[28] Van House J and Rich A 1988 *J. Electron Microsc. Tech.* **9** 209
[29] Van House J and Rich A. 1988 *Phys. Rev. Lett.* **61** 488
[30] Bauer E 1962 *Electron Microscopy* vol 1, ed. S S Breese Jr (New York: Academic) D-11
[31] Telieps W 1987 *Appl. Phys.* A **44** 55